Computational Design, Molecular Modeling and Synthesis of New 1,2,4 – Triazole Analogs with Potential Antifungal Activities

Sherin M El-Feky, Laila A Abou-Zeid[*], Mohamed A Massoud, Shady G Shokralla[1] and Hassan M Eisa

Departments of Pharmaceutical Organic Chemistry, [1]Departments of Microbiology, Faculty of Pharmacy, University of Mansoura, Mansoura 35516, Egypt

[*]Corresponding author
http://dr-lailaabouzeid-drugdiscovery.webs.com/index.htm

Abstract

A new series of triazoles were synthesized and evaluated for both antifungal and antibacterial activity. All compounds tested showed considerable antifungal activity against micromycetes, compared to the commercial fungicide, Fluconazole. Computational studies indicated that the designed compounds interact with 1EA1 enzyme active site through hydrophilic, *van der Waals* and hydrogen bond recognition. Compound **5a** performed highest antifungal activity against *C. Albicans*.

Keywords: Triazoles; Antifungal; Antibacterial; Molecular modeling; catalytic triad recognition.

Graphical Abstract: The new synthesized triazoles were evaluated for the antifungal activity and the docking studies were achieved for exploring the functional structure groups.
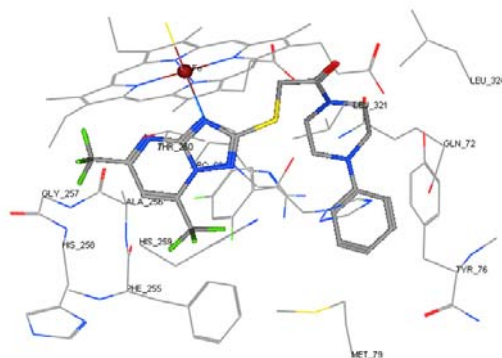
Introduction

A main impediment in the cure of Candida infections is the increase of antifungal drug battle, mainly in patients whom subjected to comprehensive antimycotic remedy [1]. Antifungal azoles are used to treat Candida infections, however although the proper antifungal activities observed in vitro, their therapeutic efficacy is variable, so that candidemia is considered as main reason of death [2]. Antimycotic medication is restricted by a number of adverse side effects [3] Antifungal drugs represent life-time maintenance therapy either against present fungal infections or as prophylactic treatment against possible fungal infections triggered the need for novel generation of selective antifungal analogs. In the present work, the authors seek developing new generation of selective antifungal agents.

The current antimicrobial drug therapies suffer drug-related toxicity, resistance and serious drug-drug interactions, triggered the need of new generations of broad spectrum antimicrobial drugs with selectivity and solution for multi-drug resistance problems. The frequency of systemic fungal infections increased significantly due to an augment in the number of immuno-compromised hosts, such as patients treated with anticancer chemotherapy or patients performed organ transplants and patients with AIDS [4]. Because of the high therapeutic index of azoles, they are considered the first-line drugs for the treatment of persistent fungal infections. Remarkably the extensive utilization of azoles has led to development of complicated resistance which drastically inferior the efficacy of them [5]. Antifungal azoles perform competitive inhibition of the lanosterol 14a-demethylase (CYP51) which is the key enzyme in sterol biosynthesis of fungi [6]. Selective inhibition of CYP51 caused exhaustion of ergosterol and accumulation of lanosterol and other 14-methyl sterols resulting in the inhibition of fungal cell growth [7]. The machinery of azoles recognition within CACYP51 pocket was investigated by computational docking and mutagenesis [8-10]. Structure-based drug design was applied to provide novel azole candidates.

Rational of the design of the target compounds

The well-known antifungal azole ergosterol biosynthesis inhibitors such as Ketoconazole and Fluconazole **(TPF)** have revolutionized treatment of some fungal infections, chart 1. These inhibitors are toxic to the liver of the host and have serious side effects due to its inhibition of other CYPs. Clinical antifungal or antibacterial inhibitors that inhibit the enzymatic activities of only fungus or bacterial CYPs without inhibition of other

CYPs from the host are desired, because for example human CYP51 is essential for human metabolism. Crossover inhibition of CYP51 in two different species still causes undesirable side effects and is one of the reasons for the continuing search for better agents. Some azoles showed selective inhibition of yeast and

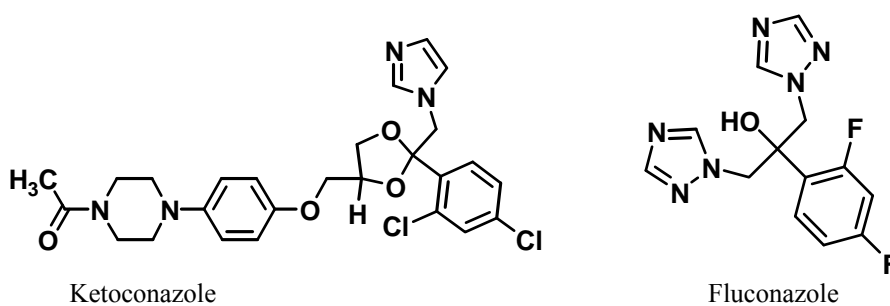Ketoconazole   Fluconazole
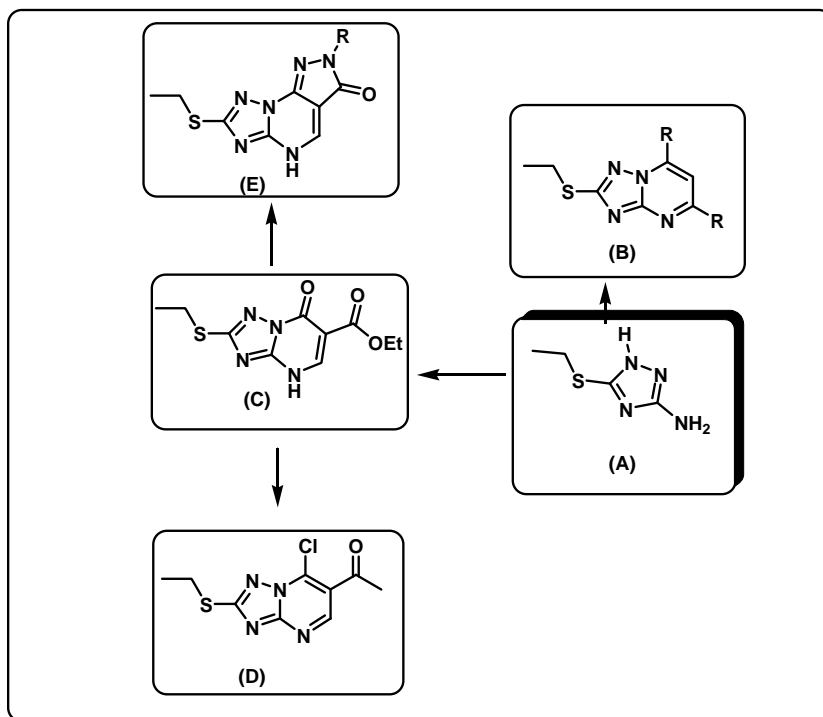
Chart 1

Chart 2

fungal CYP51 over the corresponding plant and human species. To design new azole derivatives with high specificity for bacterial and fungal CYP51s, the molecular mechanism for specificity of the inhibitor binding to CYP51s needs to be elucidated. For discovery of novel anti-fungal or anti-bacterial azoles which do not inhibit human enzymes, the detailed characterization of the structural diversities in the heme pockets between mammalian and bacterial CYP51s is essential [11].

To improve the recognition at the active site of the enzyme (CYP51) and with cellular and viral DNA, our attention focused on starting material bearing the basic skeleton of [1,2,4]-triazoles with NH_2 at C_5 and -S-CH_2- bridge at C_3 (**A**), which would offer conformational flexibility. Occlusion of (A) as a part of [1,2,4]-triazolo[1,5-*a*]pyrimidines (**B**, **C**, and **D**) and   pyrazolo[4,3-*e*][1,2,4]-triazolo[1,5-*a*]pyrimidines (**E**) were proposed to examine their vast activity, chart 2.

Structural modifications at C_5-NH_2 or extension at C_3 S-CH_2- or both together were achieved by incorporation of the essential pharmacophoric groups through formation of hydrazides, hydrazide hydrazones, Schiff bases. Piperazine ring was incorporated, as well, either through Mannich base formation or as N-acyl piperazine. These groups were expected to serve as hydrogen bond acceptor entities or hydrophobic functional groups that are important for π - π stacking with the hydrophobic amino acid residues at the binding site of the target enzyme.

The acetohydrazide derivatives of B were done (**2a,b**) and then cyclized into the corresponding [1,2,4]-triazole 3-thiol which in turn were alkylated to provide the target compounds (**3a,b**) and (**4a,b**).
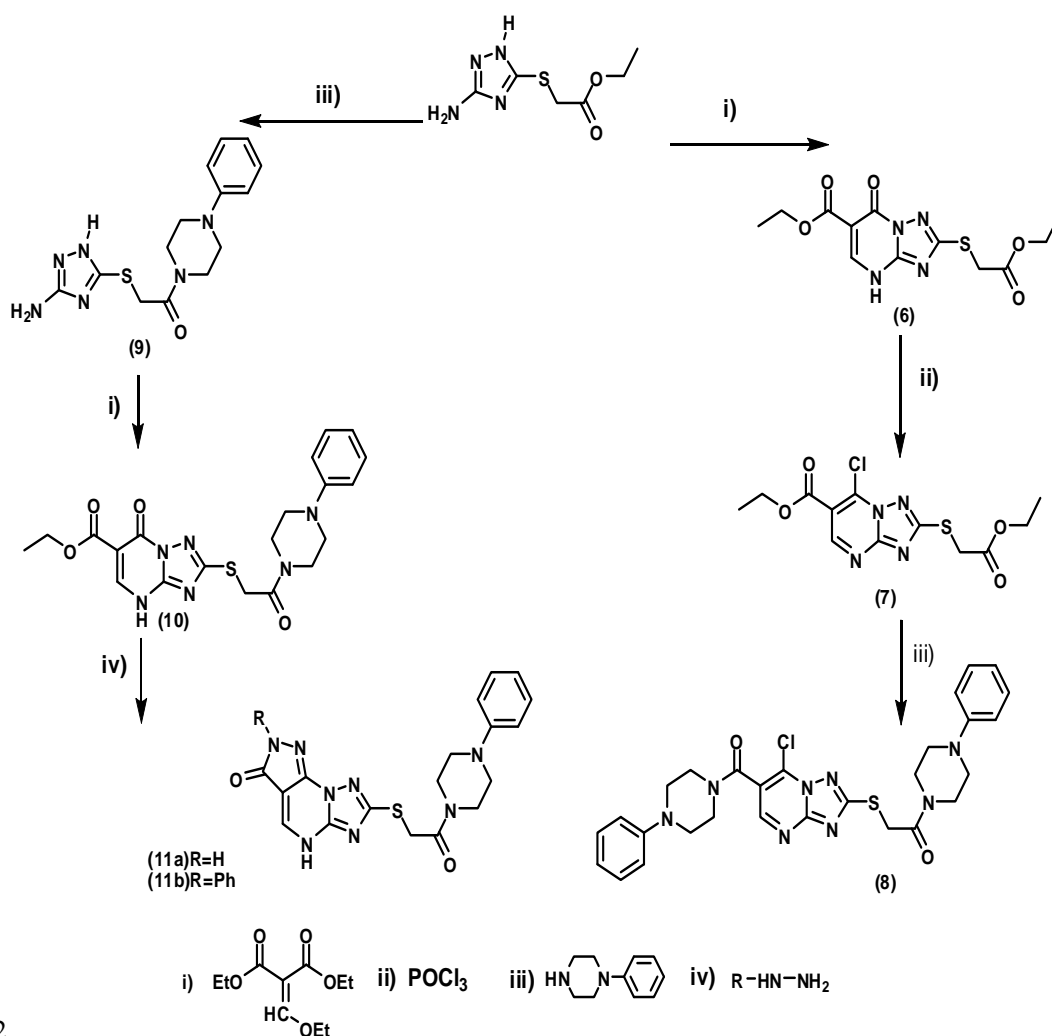
Structural modification of the triazolopyrimidine (**C**) was designed through introduction of chloro at C_7 to increase their lipid solubility and in turn increase the activity [12]. In addition, the ketoester functional moiety of (**C**) undergo cyclization with hydrazines to afford pyrazolo[4,3-e][1,2,4]-triazolo[1,5-a]pyrimidines (**E**) represented by (**11a,b**). N-aryl-N-acylpiperazine moiety was incorporated as a side chain substituents to all of (B), (C), (A) and (D) to give (**5a-c**), (**9**), (**10**) and (**8**) respectively.

Molecular Modeling Study
In the present study, synthesis of novel triazoles with a potential microbial inhibition activity was considered. The rationale behind this concept is based on the finding that synthetic triazole inhibitors be recognized at the enzyme pocket in a highly matched complementary manner to (**TPF**). The extent of complementarities (binding) of analogs with the enzyme pocket was predicted by hydrogen bonding and energy calculations.

Chemistry
Preparation of the titled compounds were accomplished as shown in scheme 1, 2. Compounds **1a,b** were prepared according to published procedures by refluxing 3-amino-5-mercapto[1,2,4]triazole with acetyl acetone or trifluoro-acetyl acetone as 1,3-dicarbonyl compound in piperidine and acetic acid [13]. Compounds **2a,b** were prepared by refluxing **1a,b** with hydrazine hydrate in absolute ethanol. Compounds **2a,b** were refluxed with 4-fluorophenyl isothiocyanate in 5% sodium hydroxide solution in aqueous ethanol to afford the corresponding 5-((5,7-disubstituted-[1,2,4]triazolo-[1,5-a]pyrimidin-2-ylthio)methyl)-4-(4-fluorophenyl)-1*H*-1,2,4-triazole-5 (4*H*)-thiones **3a,b.** Compounds **3a,b** were alkylated using the appropriate alkyl halide to afford   2-((5-(alkylthio)-4-(4-fluorophenyl)-4H-1,2,4-triazol-3-yl)methylthio)-5,7-disubstituted-[1,2,4] triazolo[1,5-a]pyrimidines **4a,b**. Compounds **1a,b** were refluxed with the appropriate piperazine derivatives to afford 2-(5,7-disubstituted-[1,2,4]triazolo[1,5-a]pyrimidin-2-ylthio)-1-(4-substituted piperazin-1-yl) ethanone

5a-c. Compound **6** was prepared by refluxing 3-amino-5-mercapto [1,2,4]triazole with diethylethoxymethylene malonate (DEEM). Compound **6** afforded chloro-derivative ethyl-7-chloro-2-(2-ethoxy-2-oxoethylthio)-[1,2,4]triazolo[1,5-a]pyrimidine-6-carboxylate, **7** by refluxing with phosphorous oxychloride using triethylamine. Compound 2-(7-chloro-6-(4-phenyl-piperazine-1-carbonyl)-[1,2,4] triazolo[1,5-a]pyrimidin-2-ylthio)-1-(4-phenylpiperazin-1-yl) ethanone, **8** was obtained by refluxing **7** with phenyl piperazine. Compound 3-amino-5-mercapto[1,2,4]triazolo was refluxed with phenyl piperazine to give 2-(3-amino-1H-[1,2,4]-triazol-5-ylthio)-1-(4-phenylpiperazin-1-yl)etha-none **9,** that was refluxed with (DEEM) to give ethyl-7-oxo-2-(2-oxo-2-(4-phenylpiperazin-1-yl)ethy lthio)-4,7-dihydro-[1,2,4]triazolo[1,5a]-pyrimidine-6-carboxylate **10**. Compounds **11a,b** was obtained by refluxing compound **9** with the appropriate hydrazine derivatives.

Scheme 2

Results and Discussion

Molecular modeling

As a reference to our modeling and docking studies, the tertiary complex of 1EA1 enzyme, coupled with

HEM and TPF as inhibitor, was used as a template [8]. Studying the triazole ring binding interaction of TPF with the 1EA1 binding active site indicated that the N_4 of the triazole ring and the carbonyl oxygen contributed preferable hydrogen bonds with the key amino residue **Cys394** and with the cofactor HEM. The N_1, N_2, N_4 atoms of the second triazole ring of TPF performed trifurcated H-bonds with the `catalytic triad' residues of 1EA1 binding site **Phe255**, **Ala256**, and **His259** respectively (fig. 1).

Molecular modeling studies of **(3a, b)** showed that the triazolopyrimidine hetero fused ring improved the

binding performance with the active site residues by forming bifurcated hydrogen bonds with the crucial residue **His259**. S at C_3 atom of the thiotriazole moiety in compounds **(3a, b)** performed bifurcated interacted with cofactor **HEM** binding pocket (fig. 2). Presence of two trifluoromethyl functional groups lead to increase of its lipophilic character to an unfavorable level (logp = 5.10), that may interfere with the expected biological activity (table 1).
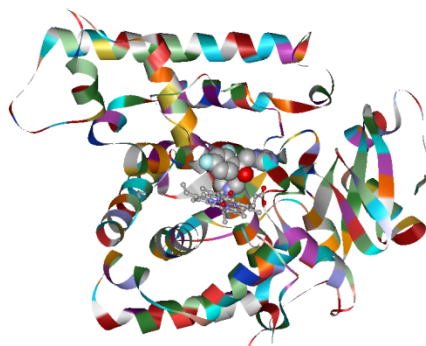

Fig. 1: Flat-ribbon presentation of the crystallographic structure of ternary complex of TPF-HEME-1EA1, showing the stick models of TPF and the cofactor HEM.
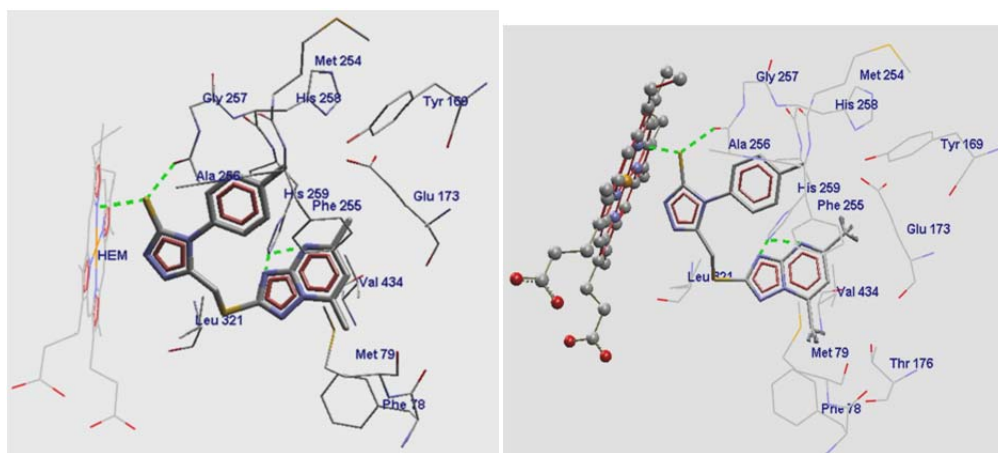

Fig. 2: Binding mode for compounds (3a, b) fitted at the 1EA1 binding pocket, showing residues involved in its recognition, dashed lines indicate the hydrogen bond formation.

In compounds **(4a, b)** the chance of hydrogen bonding with the active site residues is diminished due to the presence of hydrophobic moieties, *para*-fluorophenyl and S-benzyl, that veil the polar atoms of triazole ring. Also the hydrophobic substitutions of the triazolopyrimidine ring augment the unfavorable binding to the conserved residues. Presence of di-trifluoromethyl functional group in compound **(4b)** increases the ligand lipophilic character to an unfavorable level (logp = 5.58) that may interfere with the expected biological activity. However, N_1-atom of the triazole ring binds by chelation with the cofactor **HEM** (fig. 3).
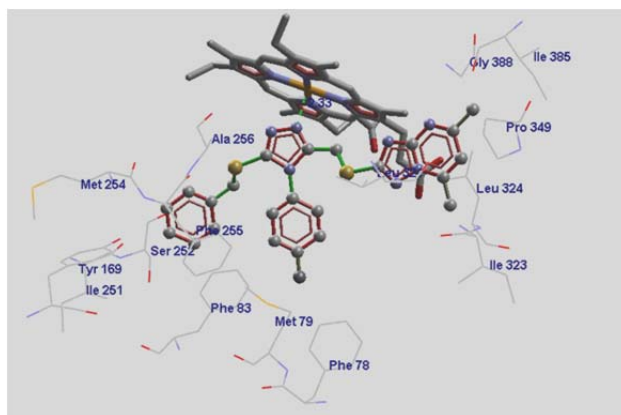
Fig. 3: Binding mode for energy minimized compound (4a) at the 1EA1 binding pocket, showing residues involved in its recognition, dashed lines indicate the hydrogen bond formation,

In compounds **(5a-c)** due to the bulkiness and the rigidity of the hydrophobic moieties, phenylpiprazine and triazolopyrimidine, which interfere with the proper conformational complementarity within the binding pocket providing a limited accommodation and in turn performed high degree of RMSD deviations that led to the orientation of the hydrophobic moieties in frontage of the hydrophobic pocket active site missing the opportunity of hydrogen bonding interaction with the surrounding conserved residues (fig. 4).

Fig. 4: Binding mode for energy minimized compounds (5a, b) docked in the 1EA1 binding pocket, showing residues involved in its recognition, dashed lines indicate the hydrogen bond formation.

Compounds **(6)** and **(7)** docked in the active site with limited conformational changes, where the two aliphatic side chains oriented too far from the amino acid residues to achieve hydrogen bonding. Moreover, the catalytic triad of the active site remains away from the hydrophobic interaction with the ligand (fig. 5).
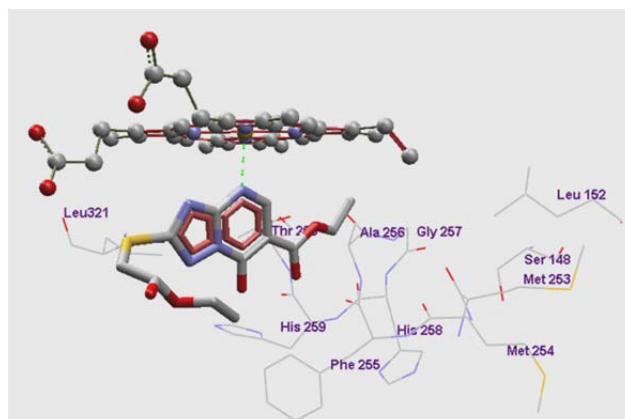
231

Fig. 5: Binding mode for compounds (6) docked and minimized in the 1EA1 binding pocket, showing residues involved in its recognition, dashed lines indicate the hydrogen bond formation.

In compound **(8)**, the existence of the two terminal phenylpiperazine groups provides flexibility for accommodation leading to proper hydrogen bonding recognition with the crucial residue **Phe255**. The stable bending conformation of compound **(8)** enhanced the binding affinity between the N_1, $N_{4'}$ atoms of triazolopyrimidine ring and the **HEM** nitrogen atoms. However the two lipophilic phenyl rings lay away from the hydrophobic pocket affording inadequate complementarity with the binding active site and missing the chance for recognition with the conserved residues that lead to a relatively inferior binding affinity (fig. 6).
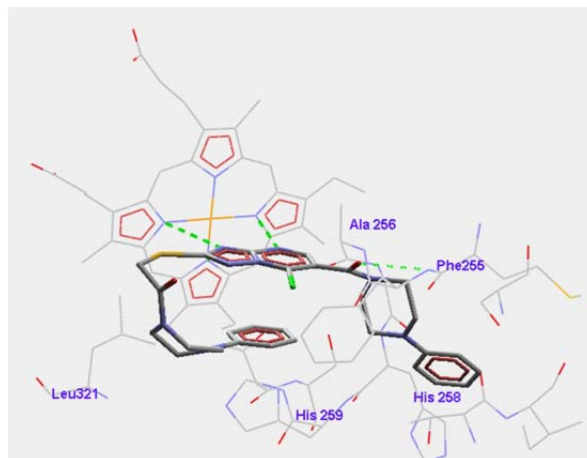

Fig. 6: Binding mode for compounds (8) optimally docked in the 1EA1 binding pocket, showing residues involved in its recognition, dashed lines indicate the hydrogen bond formation.

In compound **(9)**, the two nitrogen atoms of the piperazine ring contributed bifurcated hydrogen bonds with **Met253**. The nitrogen atom of the terminal amino group and the triazole N_4 hooked with the cofactor by three hydrogen bonds that enhance the complex stability (fig. 7).
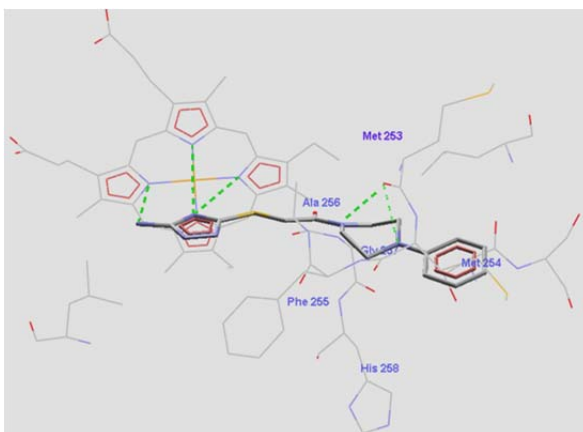
Fig. 7: Binding mode for compounds (9) optimally docked in the 1EA1 binding pocket, showing residues involved in its recognition, dashed lines indicate the hydrogen bond formation.

Comparing the performance of compounds **(5a-c)** and compound **(10)** revealed that the substitution of the triazolopyrimidine with ethyl carboxylate functional group instead of the methyl or triflouromethyl group that in their counterparts lead to favorable structural changes that allow the improving its binding affinity and electrostatic interaction within the active site. During the geometrical optimization, the ethyl carboxylate side chain was freely rotated about the torsion angle and this privilege eventually enabled the ester carbonyl oxygen to bind with the crucial residues namely **Tyr 76**. Also the carbonyl oxygen gets the chance to bind with one of the catalytic triad residues, **Ala256**. Finally, the triazolopyrimidine performed three hydrogen bonds with the nitrogen atoms of the cofactor **HEM** (fig. 8).

Fig. 8: Binding mode for compounds (10) aligned in the 1EA1 binding pocket, showing residues involved in its recognition, dashed lines indicate the hydrogen bond formation.

In compound **(11a, b)**, the existence of rigid trifused rings augmented the hindrance and restricted the conformational changes of the ligand leading to the failure of accommodation and diminution of the recognition with high degree of RMSD deviation with the surrounding residues (fig. 9).
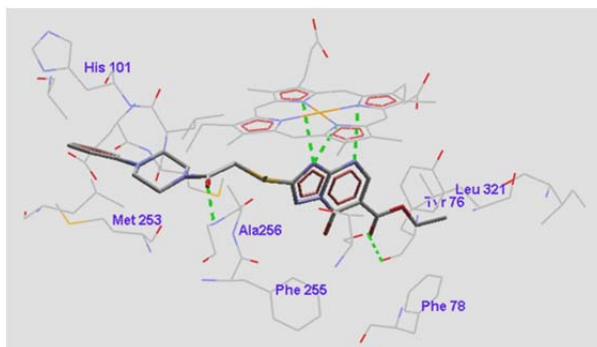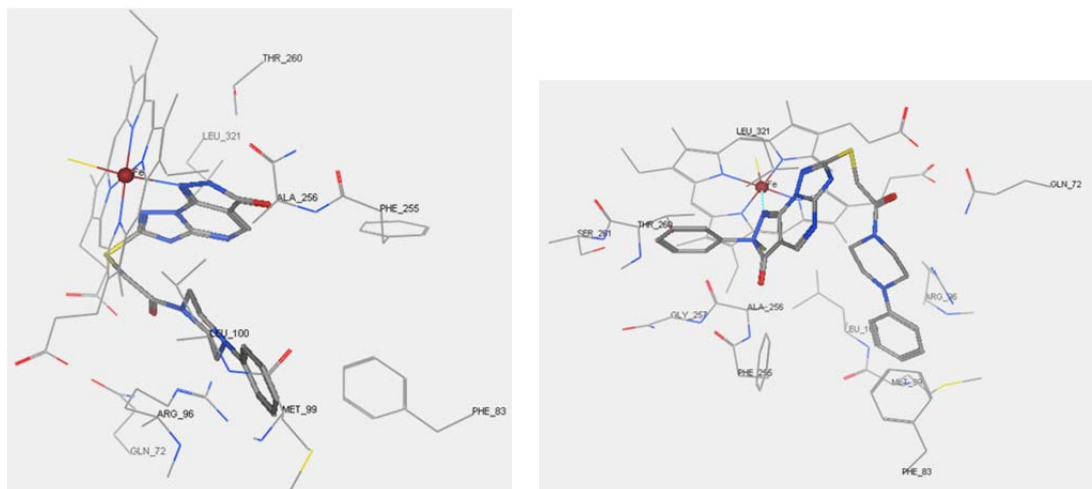
Fig. 9: Binding mode for compounds (11a, b) optimally docked in the 1EA1 binding pocket, showing residues involved in its recognition, dashed lines indicate the hydrogen bond formation.

In conclusion recognition with "catalytic triad" P**he255, Ala256** and **His259**, is essential for binding and that reflected improvement in the biological activity. The amino acid **Tyr76** is not one of the key residues for recognition of the parent ligand TPF but it is playing a crucial rule in the recognition of the tested ligands and that was designated from the elucidation of the biological data.

Structural activity relationship
The molecular docking results revealed that: i) Triazole and the fused triazolo pyrimidine rings are essential for CYP51 inhibition through their N_1, N_4 or both as recognition features with the Iron Fe atom of HEM cofactor, key amino acids residues at the enzyme pocket. ii) Ethyl carboxylate functional side chain that's freely rotated about torsion angles and that's not extended to other side chains is important for allowing carbonyl oxygen to bond with the conserved residues at the binding site. iii) Flexible thio-methylene spacer was necessary to allow hydrophobic recognition of phenyl rings with hydrophobic patch of amino acids at the enzyme pocket. iv) *Trans* conformation at carbon nitrogen double bond stabilized ligand-enzyme complex and enhanced electrostatic hydrogen bonds and hydrophobic interaction at the enzyme binding site. v) Halo-substituted phenyl rings allowed lipophilic recognition within the binding--pocket.

Pharmacophoric groups
Incorporation of essential pharmacophoric groups proved to increase the reactivity as following: 1) Mannich base analogs are biologically active due the presence of the basic function that renders the molecule soluble in aqueous solvents. They exhibit extensive activities such as antimicrobial, antiviral, as well as anticancer activities. 2) Hydrazides and hydrazide hydrazones were found to exhibit broad antimicrobial and antitumor activities. 3) Piperazine moiety is a biologically valuable moiety exhibit broad biological activity including; antiviral and anticancer activities. 4) Schiff bases derivatives of the heterocyclic triazole analogs exhibited broad biological activities including; antimicrobial activities. 5) N_4 of triazolo-ring is fundamental for the antifungal activity of Fluconazole (TPF) that N_4 coordinates with heme iron atom of CYP51 enzyme at its active site.

Antimicrobial activity
New synthesized compounds were screening for their antimicrobial activities*" in vitro".*

Activity against Staphylococcus aureus
(**3a**) showed moderate antibacterial activity against *Staphylococcus aureus* (table 1).
Table 1: Antimicrobial activity of compounds (3-11)

Comp. No.	Microorganisms		
	Gram -ve	Gram +ve	Fungi
	E.coli	*S. aureus*	*C. albicans*
3a	-	18	-
3b		-	13
4a	-	-	-
4b	-	-	-
5a	-	-	21
5b	-	-	-
5c	-	-	-
6	-	-	-
7	-	-	-
8	-	-	-
9	-	-	-
10	-	-	-
11a	-	-	14
11b	-	-	-
Ampicillin	31	23	-
Clotrimazol	-	-	40
Fluconazole	-	-	38

Degree of activity is measured by the zone of inhibition:
(-): No inhibition (resistant, not sensitive), (10-15 mm, slightly active), (15-20)
mm, moderately active), (20-25 mm, highly active), > 25 mm, very active.

Activity against fungi
Compound **5a** was highly active,Compounds **3b** and **11a** were slightly active against *Candida albicans* (table 1).
Cytotoxicity assays
The cytotoxicity assay using (EAC) assay showed low % of viability for all the tested compounds indicating that they have high cytotoxicity against (EAC) (table 2). The cytotoxicity assay using Bleomycine –dependant DNA damage assay showed that only **5a**, **10** and **11a** can bind with and protect DNA (table 3).
Table 2: Viability of Earlich Ascitis Carcinoma cells

Comp. No	EAC % viability
3a	1
3b	2
5a	5
5c	4
6	4
7	3
8	2
10	5
11b	3

Table 3: Degree of DNA damage

Comp. No.	Bleomycine dependant DNA damage assay (A)
3a	0.123
3b	0.101
5a	0.092
5c	0.202
6	0.101
7	0.160
8	0.119
10	0.095
11b	0.097

Conclusion

The compound with the highest antifungal activities was **5a** that exhibited piperazine moiety. All the compounds showed low % of viability with high cytotoxicity.

Experimental

Computational Molecular Modeling methodology

All modeling experiments were conducted with Hyperchem 6.03 package and Moelgro package ([16-17].

Enzyme structure

The 1EA1 enzyme in tertiary complex with protoporphyrin IX containing Fe (**HEM**) and (**TPF**), code ID 1EA1, was downloaded from the "Protein Data Bank", (fig. 1).

Building up the 3D Structure of the synthesized triazoles

The triazole analogs **3-11** were assembled from fragment libraries of the software. The partial atomic charges for each analog were assigned with the semiemperical method "AM1". Energy minimization was applied using the "Amber force field". Conformational search was performed the rotatable bonds using an increment of 10. The global minima of each candidate was used for docking studies.

Docking and Molecular geometrical optimization

Each new analog "global-minima" was docked into the 1EA1 enzyme-binding pocket. For each traizole analog, energy optimization was performed using Amber force field till reach a RMS energy gradient of 0.01 Kcal/mol Å. Hydrogen bonds with a bond length up to 3.5 Å were considered. The active site of the enzyme was defined. The cofactor (**HEM**) as a part of the enzyme structure was flexible during the geometrical optimization.

Antimicrobial screening

Disc diffusion assay

Disc diffusion assay was performed according to the published procedures [14-15]. Whatman filter paper discs of 5 mm diameter were sterilized with autoclave for 15 minutes at 120°C. The sterile discs were soaked with the test compounds (500 μg/ disc). Agar plates were prepared by pouring a suitable volume of melted nutrient agar into each 75 mm Petri plates. The volume of nutrient agar was enough to keep its depth at approximately 6 mm. The agar plates were surface inoculated with standard inoculums (10^5 cells/ml broth) of the test organisms (local strains) namely, *Staphylococcus aureus*, *Escherichia coli* and *Candida albicans*. The impregnated discs were placed on the agar plate medium, suitably spaced apart and the plates were incubated

at 5°C for one hour to permit diffusion and incubated at 37°C for 24 hours for bacterial growth and at 28°C for 72 hours for fungal increment.

Cytotoxicity assays
Nine of the newly synthesized triazolopyrimidines were screened as cytotoxic against using:

Ehrlich cells
(Ehrlich Ascitis Carcinoma, EAC) derived from ascetic fluid from diseased mouse (purchased from National Cancer institute, Cairo, Egypt). The cells were grown in floating suspension culture in RPMI 1640 medium, supplemented with 10% foetal bovine serum. They were maintained at 37^0C in a humidified atmosphere with 5% CO2. The percentage viability of the cells was determined using: trypan blue DMSO was used as negative control where the viability of cells in control experiments reached 95%. Test compounds were prepared initially at concentration 1mg/ml DMSO. The % viability is listed in (table 2).
Bleomycine –dependant DNA damage assay
L-ascorbic acid, ethylenediaminetetracetic acid (EDTA), thiobarbituric acid (TBA) and bleomycin sulphate were all purchased Aldrich Co., USA. Magnesium chloride, ferric chloride and hydrochloric acid of high analytical grade from ELNasr Co. for pharmaceutical chemicals, Egypt. The reaction mixture contained DNA (0.5 mg/ml), bleomycin sulfate (0.05 mg/ml), MgCl2 (5 mM), FeCl3 (50 µM) and samples were tested in a ure was incubated at 37 ^{0}C for one hour. The reaction was completed by adding 0.05 ml EDTA concentration of 0.1 mg/ml. L-ascorbic acid (0.1 mg/ml) was used as positive control. The mixture was incubated at 37 ^{0}C for one hour. The reaction was completed by adding 0.05 ml EDTA (0.1 ml). Color was generated due to the addition of 0.5 ml thiobarbituric acid (TBA) (1% w/v) and 0.5 ml HCl (25% v/v) followed by heating at 80 ^{0}C for 10 minutes. After centrifugation, the DNA damage was measured according to the absorbance increment records. The degree of DNA damage described in terms of sample absorbance (A) is listed in table 3.

Experimental
General procedure for the synthesis of ethyl 2-(5,7-disubstituted-[1,2,4]triazolo[1,5-a]pyrimidin-2-ylthio)acetate (1a, b)
A mixture of ethyl 2-(3-amino-1*H* –[1,2,4]-triazol-5-ylthio) acetate (3g, 0.01 mol) , acetyl acetone (1 g, 0.01 mol) or hexaflouro acetyl acetone (2.08 g, 0.01 mol) and 0.1ml pipridine in 40ml acetic acid was refluxed.. The reaction mixture was evaporated under *vacuum* and the obtained residue was stirred with ice-water. The separated precipitate was recrystallized from ethanol to yield the corresponding compounds 1a,b.

Ethyl 2-(5,7-dimethyl -[1,2,4]-triazolo[1,5-a]pyrimidin -2-ylthio) acetate (1a):
Yield: 90%; M.P 140-142 ^{0}C (Yang *et al.,* 2002: M.P 142-143 ^{0}C).

Ethyl 2-(5,7-bis(trifluoromethyl)-[1,2,4]-triazolo[1,5-a]pyrimidin-2-ylthio) acetate (1b):
Yield: 88%; M.P 70-73 ^{0}C (Yang *et al.,* 2002).

General procedure for the synthesis of 2-(5,7-disubstituted-[1,2,4]triazolo[1,5-a]pyrimidin-2-ylthio)acetohydrazide (2a,b):
A mixture of alcoholic solution of ethyl2-(5,7-disubstituted-[1,2,4]triazolo[1,5-a]pyrimidin-2-ylthio) acetates **(1a,b)** and hydrazine hydrate was refluxed and the separated white crystalline precipitate of the target hydrazide was recrystallized from ethanol to yield the corresponding compounds 2a,b.

2-(5,7-Dimethyl- [1,2,4]-triazolo[1,5-a]pyrimidin-2-ylthio) acetohydrazide (2a)

Yield: 88%; M.P 195-200 ^{0}C (Yang *et al.,* 2002: yield: 93%: M.P 201-203 ^{0}C).

2-(5,7-Bis (trifluoromethyl) -[1,2,4]-triazolo[1,5-a]pyrimidin-2-ylthio) acetohydrazide (2b)

Yield: 90%; M.P 133-135 ^{0}C (Yang *et al.,* 2002).

General procedure for the synthesis of 3-((5,7-disubstituted-[1,2,4]triazolo[1,5-a]pyrimidin-2-ylthio)methyl)-4-(4-fluorophenyl)-1*H*-1,2,4-triazole-5(4*H*)-thione (3a,b)

Mixtures of 2-(5,7-disubstituted-[1,2,4]triazolo[1,5-*a*]pyrimidin-2-ylthio) acetohydrazide **(2a,b)** (0.003mol) and 4-flourophenylisothiocyanate (0.6g, 0.003 mol) in 5% ethanolic sodium hydroxide solution were refluxed and monitored with TLC for 24hrs. The ethanolic solutions were evaporated under vacuum. The remaining residues were washed with water. The aqueous filtrates were neutralized with few drops of Conc. HCl till the pH 5-6. The buff precipitates produced were filtered and crystallized from methanol.

3-((5,7-Dimethyl-[1,2,4]triazolo[1,5-a]pyrimidin-2-ylthio)methyl)-4-(4-fluorophenyl)-1*H*-[1,2,4]-triazole-5(4*H*)-thione (3a)

Yield: 70%; M.P 86-89 ^{0}C; ^{1}H NMR (DMSO-d6) δ in ppm 2.5 (s,6H ,CH$_3$), 4.5 (s ,2H,CH$_2$), 6.6-7.1 (m,5H;4H Ar,1H hetero), 14.5 (s,1H,NH). Anal. Calcd for C$_{16}$H$_{14}$FN$_7$S$_2$; C, 49.60; H, 3.64; N, 25.31. Found: C, 49.22; H, 4.12; N, 25.74.

 3-((5,7-Bis(trifluoromethyl)-[1,2,4]triazolo[1,5-a]pyrimidin-2-ylthio)methyl)-4-(4-fluorophenyl)-1*H*-[1,2,4]-triazole-5(4*H*)-thione (3b)

Yield: 78%; M.P 91-94^{0}C; ^{1}H NMR (DMSO-d6) δ in ppm 4.4 (s,2H,CH$_2$), 6.4-7.5 (m,5H,4H Ar, 1Hhetero), 14.7 (s,1H,NH). Anal. Calcd for C$_{16}$H$_8$F$_7$N$_7$S$_2$; C, 38.79; H, 1.63; N, 19.79. Found: C, 39.12; H, 2.44; N, 20.13.

General procedure for the synthesis of 2-((5-(alkyl thio)-4-(4-fluorophenyl)-4*H*-1,2,4-triazol-3-yl)methyl-thio)-5,7-disubstituted-[1,2,4]triazolo[1,5-a]pyrimidine (4a, b)

Solutions of equimolar amounts of (0.002mol) of each of 5-((5,7-disubstituted- [1,2,4]-triazolo-[1,5-*a*]-pyrimidin-2-ylthio)-methyl)- 4-(4-fluoro- phenyl)-4*H*-1,2,4-triazole-3-thiol (**3a,b**), benzyl chloride (3g) or ethyl iodide (0.31g) and potassium carbonate (0.3g) in DMF were stirred at 80 ^{0}C. The reaction was monitored with TLC to yield (**4a**,**b**). The reaction mixtures were evaporated under vacuum and the obtained residue was crystallized from ethanol.

2-((5-(benzylthio)-4-(4-fluorophenyl)-4*H*-[1,2,4]-triazol-3-yl)methylthio)-5,7-dimethyl-[1,2,4]triazolo[1,5-a]pyrimidine (4a)

Yield: 70% (ethanol); M.P 160-162 ^{0}C; ^{1}H NMR (DMSO-d6) δ in ppm 2.4 (s,6H,CH$_3$), 4.6 (s,4H,CH$_2$), 6.8 (s,1H,CH$_2$), 7.1-7.5 (m,9H, Ar). Anal. Calcd for C$_{23}$H$_{20}$FN$_7$S$_2$; C, 57.84; H, 4.22; N, 20.53. Found: C, 58.11; H, 4.75; N, 20.14.

2-((5-(ethyl thio)-4-(4-fluorophenyl)-4*H*-[1,2,4]-triazol-3-yl)methylthio)-5,7- bis(trifluoromethyl)-[1,2,4] triazolo [1,5-a]pyrimidine (4b)

Yield: 68% (aq.ethanol); M.P 77-80 ^{0}C; ^{1}H NMR (DMSO-d6) δ in ppm 1.5 (t,3H,CH$_3$) ,3.4 (q,2H,CH$_2$) ,4.5 (s, 2H,CH$_2$), 6.8-7.5 (m,5H,4H Ar,1H hetero). Anal. Calcd for C$_{18}$H$_{12}$F$_7$N$_7$S$_2$; C, 41.30, H, 2.31, N,18.73. Found: C, 41.67, H, 2.55, N, 18.33.

General procedure for the synthesis of 2-(5,7-disubstituted-[1,2,4]triazolo[1,5-a]pyrimidin-2-ylthio)-1-(4-phenylpiperazin-1-yl) ethanone(5a-c)

To solutions of ethyl 2-(5,7-disubstituted-[1,2,4]triazolo[1,5-*a*]pyrimidin-2-ylthio) acetate **(1a,b)** (0.003mol) in phenyl piprazine (1.8g, 0.03 mol) in glacial acetic acid or hydrochloride salt of p-tolylpiprazine (0.56g, 0.002mol) was added drop wise. The reaction mixtures were refluxed and monitored with TLC. The solutions were concentrated using vacuum. The residues were treated with ice-water. The formed precipitates were filtered and crystallized from aqueous ethanol.

2-(5,7-Dimethyl-[1,2,4]triazolo[1,5-a]pyrimidin-2-ylthio)-1-(4-phenylpiperazin-1-yl) ethanone (5a)

Yield: 88%; M.P 143-145 ^{0}C; ^{1}H NMR (DMSO-d6) δ in ppm 2.4 (s,3H,CH$_3$), 2.7 (s,3H,CH$_3$), 3.0 (t,4H,CH$_2$), 3.1 (t,4H,CH$_2$), 3.6 (s,2H,CH$_2$), 6.7-7.2 (m, 6H,5HAr,1H hetero) . Anal. Calcd for C$_{19}$H$_{22}$N$_6$OS; C, 59.66, H, 5.80, N, 21.97. Found: C, 59.22, H, 5.80, N, 21.87.

2-(5,7-Bis(trifluoromethyl)-[1,2,4]triazolo[1,5-a]pyrimidin-2-ylthio)-1-(4-phenylpiperazin-1-yl) ethanone (5b)

Yield: 90%; M.P 88-90^{0}C; ^{1}H NMR (DMSO-d6) δ in ppm 4.0 (m,4H,CH$_2$), 4.1(m,4H,CH$_2$), 4.2 (s,2H,CH$_2$), 6.2-7.4 (m,6H, 5HAr,1H hetero). Anal. Calcd for C$_{19}$H$_{16}$F$_6$N$_6$OS; C, 46.53, H, 3.29, N, 17.14. Found: C, 46.23, H, 3.74, N, 16.90.

2-(5,7-Bis(trifluoromethyl)-[1,2,4]triazolo[1,5-a]pyrimidin-2-ylthio)-1-(4-p-tolylpiperazin-1-yl) ethanone (5c)

Yield: 91%; M.P 247-250 ^{0}C; ^{1}H NMR (DMSO-d6) δ in ppm 2.4 (s,3H,CH$_3$), 4.0 (m,4H,CH$_2$), 4.1(m,4H,CH$_2$), 4.2 (s,2H,CH$_2$), 6.7-8.3 (m,6H,5HAr,1Hhetero). Anal. Calcd for C$_{20}$H$_{18}$F$_6$N$_6$OS; C, 47.62, H, 3.60, N, 16.66. Found: C, 47.42, H, 3.23, N, 16.43.

Ethyl 2-(2-ethoxy-2-oxoethylthio)-7-oxo-4,7-dihydro-[1,2,4]triazolo[1,5-a]pyrimidine-6-carboxylate (6)

Mixture of diethyl ethoxymethylenemalonate (DEEM) (0.32g, 0.004 mol) and acidic solution of ethyl 2-(3-amino-1*H*–[1,2,4]-triazol-5-ylthio) acetate (2g, 0.025mol) was refluxed, evaporated under vacuum and the separated residue was crystallized.

Yield: 83% (aq. Ethanol); M.P 175-180 ^{0}C; ^{1}H NMR (DMSO-d6) δ in ppm 1.3 (t,6H,CH$_3$), 4.2 (q,4H,CH$_2$), 4.25 (s,2H,CH$_2$), 6.1 (s,1H,NH), 8.5 (s,1H,hetero). Anal. Calcd for C$_{12}$H$_{14}$N$_4$O$_5$S; C, 44.17, H, 4.32, N, 17.17. Found: C, 44.63, H, 4.11, N, 16.82.

Ethyl 7-chloro-2-(2-ethoxy-2-oxoethylthio)-[1,2,4] triazolo[1,5-a]pyrimidine-6-carboxylate (7)

A solution of ethyl 2-(2-ethoxy-2-oxoethylthio)-7-oxo-4,7-dihydro-[1,2,4-a] pyrimidine-6-carboxy-late **(6)** (0.33g, 0.001mol), (10ml) of phosphorous oxychloride and triethyl amine was refluxed for 6hrs. By cooling the reaction mixture, the precipitate was obtained, filtered and recrystallized.

Yield: 56% (aq. ethanol); M.P 147-150 ^{0}C; ^{1}H NMR (DMSO-d6) δ in ppm 1.4 (t,6H,CH$_3$) , 4.1 (q,4H,CH$_2$),4.5 (s,2H,CH$_2$), 6 (s,1H,NH),8.8(s,1H,CH). Anal. Calcd for C$_{12}$H$_{13}$ClN$_4$O$_5$S; C, 41.80, H, 3.80, N, 16.25. Found: C, 41.54, H, 4.11, N,16.83.

2-(7-chloro-6-(4-phenylpiperazine-1-carbonyl)-[1,2,4]triazolo[1,5-a]pyrimidin-2-ylthio)-1-(4-phenylpiperazin-1-yl) ethanone (8)

Phenyl piprazine (2 g, 0.01 mol) was added dropwise to a stirred solution of ethyl 7-chloro-2-(2-ethoxy-2-oxoethylthio)-[1,2,4]triazolo[1,5-a]pyrimidine-6-carbo-xylate **(7)** (0.5 g, 0.001 mol) in toluene (25 ml). The reaction mixture was refluxed for 24 hours. The reaction mixture was evaporated under vacuum. The collected residue crystallized from aqueous ethanol.

Yield: 72% (aq. ethanol); M.P >300^{0}C; ^{1}H NMR (DMSO-d6) δ in ppm 3.35(m,8H,CH$_2$), 3.58(m,8H,CH$_2$), 4.41 (s,2H,CH$_2$), 6.58.6 (m,11H,10HAr,1H hetero). Anal. Calcd for C$_{28}$H$_{29}$ClN$_8$O$_2$S; C, 58.27, H, 5.07, N, 19.42. Found: C, 58.54, H, 5.55, N,19.81.

2-(3-amino-1*H*-[1,2,4]-triazol-5-ylthio)-1-(4-phenyl-piperazin-1-yl) ethanone (9)

Ethyl 2-(3-amino-1H-[1,2,4]-triazol-5-ylthio) acetate (2g, 0.001 mol) was dissolved in glacial acetic acid (20 ml) and mixed under reflux with a solution of phenyl piprazine (3.2g, 0.002 mol) in glacial acetic acid for 48 hrs. The reaction mixture was evaporated and the residue was crystallized.

Yield: 66% (ethanol); M.P 145-148 ^{0}C; ^{1}H NMR (DMSO-d6) δ in ppm 3.2(m,4H,CH$_2$), 3.4(m,4H,CH$_2$), 3.8(S,2H,CH$_2$), 6.0(s,2H,NH), 6.6-7.4(m,5H,Ar), 11.8(s,1H,NH). Anal. Calcd for C$_{14}$H$_{18}$N$_6$OS; C, 52.81, H, 5.70, N, 26.39. Found: C, 52.81, H, 6.13, N, 25.89.

Ethyl7-oxo-2-(2-oxo-2-(4-phenylpiperazin-1-yl)ethyl-thio)-4,7-dihydro-[1,2,4]triazolo[1,5-a]pyrimidine-6-carboxylate (10)

Reflux a mixture of diethyl ethoxymethylenemalonate (DEEM) (4.32g, 0.004 mol) and a glacial acetic acid solution of 2-(3-amino-1*H*-[1,2,4]-triazol-5-ylthio)-1-(4-phenylpiperazin-1-yl) ethanone **(9)** (4 g, 0.025 mol) was proceeded. The reaction mixture was evaporated and the afforded residue was crystallized.

Yield: 55% (ethanol); M.P >300^{0}C; ^{1}H NMR (DMSO-d6) δ in ppm 1.5(t,6H,CH$_3$) 3.3(t,4H,CH$_2$), 3.5(t,4H,CH$_2$), 4.5 (q, 4H,CH$_2$),4.7 (s,2H ,CH$_2$), 6 (s,1H,NH), 6.6-8.3(m, 6H; 5HAr,1H hetero). Anal. Calcd for C$_{20}$H$_{22}$N$_6$O$_4$S; C, 54.29, H, 5.01, N, 18.99. Found: C, 54.77, H,4.86, N, 19.32.

7-(2-oxo-2-(4-phenylpiperazin-1-yl)ethylthio)-2*H*-pyrazolo[4,3-e][1,2,4]triazolo[1,5-a]pyrimidin-3(5*H*)-one (11a)

Drop wise addition of hydrazine hydrate (1.1g, 0.02mole) to a stirred solution of ethyl 7-oxo-2-(2-oxo-2-(4-phenylpiperazin-1-yl)ethylthio)-4,7-dihydro-[1,2,4] triazolo[1,5-a]pyrimidine-6-carboxylate **(10)** (1 g, 0.002 mole) in absolute ethanol (10 ml) was performed over a period of 15 min. The reaction mixture was refluxed for 48 hours and then concentrated under vacuum. The obtained precipitate was filtered and crystallized.

Yield: 45% (ethanol); M.P >300^{0}C; ^{1}H NMR (DMSO-d6) δ in ppm 3.4 (t,4H,CH$_2$), 3.6 (t,4H,CH$_2$), 4.0 (s,1H,NHpyrimidine), 4.8 (S,2H,CH$_2$), 6.2 (s,1H,NH), 6.6-7.4 (m,5H,Ar), 9.0(s,1H,NHpyrazolo). Anal. Calcd for C$_{18}$H$_{18}$N$_8$O$_2$S; C, 52.67, H, 4.42, N, 27.30. Found: C, 52.11, H, 4.56, N, 27.67.

7-(2-oxo-2-(4-phenylpiperazin-1-yl)ethylthio)-2-phe-nyl-2*H*-pyrazolo[4,3-e][1,2,4]triazolo[1,5-a]pyrimidin-3(5*H*)-one (11b)

Ethyl 7-oxo-2-(2-oxo-2-(4-phenylpiperazin-1-yl) ethy-lthio)-4,7-dihydro-[1,2,4]triazolo [1,5-a] pyramidine-6-carboxylate **(10)** (1.5g, 0.03mol) in absolute ethanol was added to a stirred solution of phenyl hydrazine (3.7

g, 0.03mol). The reaction mixture was refluxed overnight. The excess solvent was evaporated under vacuum and the formed precipitate was crystallized.

Yield: 64% (ethanol); M.P 75-80^{0}C; ^{1}H NMR (DMSO-d6) δ in ppm 3.4(t,4H,CH$_2$), 3.6(t,4H,CH$_2$), 4.0(s,1H,NHpyrimidine), 4.8(S,2H,CH$_2$), 6.6-7.9(m,10H,Ar), 9.0(s,1H,CH). Anal. Calcd for C$_{24}$H$_{22}$N$_8$O$_2$S; C, 59.25, H, 4.56, N, 23.03. Found: C, 59.67, H, 5.12, N, 23.48.

References

1. Prasad R and Kapoor K. Multidrug resistance in yeast Candida. *Int. Rev. Cytol.*, **242**: 215-248, 2005.

2. Riccardi G, Pasca MR and Buroni S. Mycobacterium tuberculosis: drug resistance and future perspectives. *Future Microbiol.*, **4**: 597-614, 2009.

3. Belmares J, Detterline S, Pak JB and Parada JP. Corynebacterium endocarditis species-specific risk factors and outcomes. *BMC Infect. Dis.*, **7**: 4-7, 2007.

4. Chang A, Neofytos D and Horn D. Candidemia in the 21st Century. *Future Microbiology*, **3**: 463-472, 2008.

5. Moyssakis I, Vassilakopoulos TP, Sipsas NV, Perakis A, Petrou A, Kosmas N and Pangalis GA. Reversible dilated cardiomyopathy associated with amphotericin B treatment. *Int. J. Antimicrob. Agents,* **25**: 444-447, 2005.

6. Podust L., Poulos TL and Waterman MR. Crystal structure of cytochrome P450 14α-sterol demethylase (CYP51) from Mycobacterium tuberculosis in complex with azole inhibitors. *Proc. Natl. Acad. Sci. USA.* **98**: 3068–3073, 2001.

7. Foroumadi A, Ghodsi S, Emami S, Najjari S, Samadi N, Faramarzi MA, Beikmohammadi L, Shirazi FH and Shafiee A. Synthesis and antibacterial activity of new fluoroquinolones containing a substituted N-(phenethyl)piperazine moiety. *Bioorg. Med. Chem. Lett.,* **16**: 3499-3503, 2006.

8. Giraud F, Guillon R, Logé C, Pagniez F, Picot C, Le Borgne M and Le Pape P. Synthesis and structure-activity relationships of 2-phenyl-1-[(pyridinyl- and piperidinylmethyl)amino]-3-(1H-1,2,4-triazol-1-yl)propan-2-ols as antifungal agents. *Bioorg. Med. Chem. Lett.*, **19**: 301-4, 2009.

9. Sheng C, Zhang W, Zhang M, Song Y, Ji H, Zhu J, Yao J, Yu J, Yang S, Zhou Y, Zhu J and Lu J. Homology modeling of lanosterol 14alpha-demethylase of Candida albicans and Aspergillus fumigatus and insights into the enzyme-substrate Interactions. *J. Biomol. Struct. Dyn.*, **22**: 91-99, 2004.

10. Sheng C, Zhang W, Ji H, Zhang M, Song Y, Xu H, Zhu J, Miao Z, Jiang Q, Yao J, Zhou Y, Zhu J and Lü J. Structure-based optimization of azole antifungal agents by CoMFA, CoMSIA, and molecular docking. *J. Med. Chem.*, **49**: 2512-2525, 2006.

11. Dunford AJ, Neeli R, Driscoll MD, Munro AW and McLean KJ. Structure, function and drug targeting in Mycobacterium tuberculosis cytochrome P450 systems. *Arch. Biochem. Biophys.*, **464**: 228-240, 2007.

12. Liu X, Xu W and Wu J. Synthesis of 4-Amino-5-furyl-2-yl-4H-1, 2, 4-triazole-3-thiol derivatives as a Novel Class of Endothelin(ET) Receptor Antagonists *Chin. Chem. Lett.,* **14**: 790-799, 2003.

13. Chen Q, Lei X, Jiang L, Liu Z and Yang G. Synthesis, antifungal activity and CoMFA analysis of novel 1,2,4-triazolo[1,5-a]pyrimidine derivatives. *Eur. J. Med. Chem.*, **43:** 595-603, 2008.

14. Varanasi N, Baskaran I, Alangaden G, Chandrasekar P and Manavathu EK. Novel effect of voriconazole on conidiation of Aspergillus species. *Int. J. Antimicrob. Agents,* **23:** 72-79, 2004.

15. Xu J, Onyewu C, Yoell HJ, Ali RY, Vilgalys RJ and Mitchell TG. Dynamic and heterogeneous mutations to fluconazole resistance in Cryptococcus neoformans. *Antimicrob. Agents Chemother.*, **45:** 420-427, 2001.

16. Hyperchem: Molecular Modeling System, Hypercube, Inc., 1999. Release 6, Florida.

17. Moelgro Molecular Viewer MMV 2008.

Authors Column

Laila A Abou-Zeid did Ph.D. in Medicinal Chemistry in April 1995 after receiving a Pre-doctoral Scholarship for Ph.D. at Medical College of Georgia, Augusta, Georgia, USA according to the Joint Supervision Program.
She is leading a research group in topic of Drug Design and Molecular Modeling and working on computational modeling, designing and synthesis series of novel leads as selective telomerase inhibitors, the hallmark of cancer.
Laila A Abou-Zeid is member of the Editorial Board, International Journal of Chemistry, Canada and Journal of Research of Pharmaceutical, Biological Sciences, USA